The American Journal of Pathology, Vol. 184, No. 6, June 2014

ELSEVIER

The American Journal of
PATHOLOGY
ajp.amjpathol.org

ANIMAL MODELS

Laminin α1 Regulates Age-Related Mesangial Cell Proliferation and Mesangial Matrix Accumulation through the TGF-β Pathway

Liang Ning,* Hidetake Kurihara,† Susana de Vega,* Naoki Ichikawa-Tomikawa,*‡ Zhuo Xu,* Risa Nonaka,* Saiko Kazuno,§ Yoshihiko Yamada,¶ Jeffrey H. Miner,‖ and Eri Arikawa-Hirasawa*,**

From the Research Institute for Diseases of Old Age, the Departments of Anatomy and Life Structure† and Neurology,** and the Division of Proteomics and Biomolecular Science,§ the BioMedical Research Center, Juntendo University Graduate School of Medicine, Tokyo, Japan; the Department of Basic Pathology,‡ Fukushima Medical University School of Medicine, Fukushima, Japan; the National Institute of Dental and Craniofacial Research,¶ National Institutes of Health, Bethesda, Maryland; and the Renal Division,‖ Department of Internal Medicine, Washington University School of Medicine, St. Louis, Missouri

Accepted for publication February 18, 2014.

Address correspondence to Eri Arikawa-Hirasawa, M.D., Ph.D., Research Institute for Diseases of Old Age, Juntendo University Graduate School of Medicine, 2-1-1, Hongo, Bunkyo-ku, Tokyo 113-8421, Japan. E-mail: ehirasaw@juntendo.ac.jp.

Laminin α1 (LAMA1), a subunit of the laminin-111 basement membrane component, has been implicated in various biological functions *in vivo* and *in vitro*. Although LAMA1 is present in kidney, its roles in the kidney are unknown because of early embryonic lethality. Herein, we used a viable conditional knockout mouse model with a deletion of *Lama1* in the epiblast lineage (*Lama1*^{CKO}) to study the role of LAMA1 in kidney development and function. Adult *Lama1*^{CKO} mice developed focal glomerulosclerosis and proteinuria with age. In addition, mesangial cell proliferation was increased, and the mesangial matrix, which normally contains laminin-111, was greatly expanded. *In vitro*, mesangial cells from *Lama1*^{CKO} mice exhibited significantly increased proliferation compared with those from controls. This increased proliferation was inhibited by the addition of exogenous LAMA1-containing laminin-111, but not by laminin-211 or laminin-511, suggesting a specific role for LAMA1 in regulating mesangial cell behavior. Moreover, the absence of LAMA1 increased transforming growth factor (TGF)-β1—induced Smad2 phosphorylation, and inhibitors of TGF-β1 receptor I kinase blocked Smad2 phosphorylation in both control and *Lama1*^{CKO} mesangial cells, indicating that the increased Smad2 phosphorylation occurred in the absence of LAMA1 via the TGF-β1 receptor. These findings suggest that LAMA1 plays a critical role in kidney function and kidney aging by regulating the mesangial cell population and mesangial matrix deposition through TGF-β/Smad signaling. *(Am J Pathol 2014, 184: 1683—1694; http://dx.doi.org/10.1016/j.ajpath.2014.02.006)*

Laminins comprise a family of heterotrimeric extracellular matrix (ECM) proteins consisting of α, β, and γ chains[1,2] that regulate cell attachment, proliferation, and differentiation.[3,4] During early embryogenesis, laminin α1 (LAMA1) first appears at the 16-cell stage and is later present in the two basement membranes (BMs) formed before gastrulation, the embryonic BM, and Reichert's membrane. In the developing kidney, temporal changes in laminin isoform expression occur as formation of glomeruli, the filtering unit of the kidney, proceeds. The earliest precursor of the glomerular BM (GBM) contains laminin-111 (LM-111; α1β1γ1). In contrast, the GBM contains LM-521 (α5β2γ1) at later developmental stages and in adulthood. Although LAMA1 is absent from the mature GBM, it is present in the glomerular mesangial matrix, an amorphous matrix made by mesangial cells that is one of the few prominent sites in which laminins are present outside of a definitive BM.[5] The glomerular capillary wall consists of podocytes with

Supported by a Ministry of Education, Culture, Sports, Science, and Technology (MEXT), Japan, Grant-in-Aid for Young Scientists (B) 24790860 (L.N.) and grants 17082008 and 2230023 (E.A.-H.), NIH Intramural Program of the National Institute of Dental and Craniofacial Research grant (Y.Y.), NIH grant R01DK078314 (J.H.M.), and MEXT—Supported Program for the Strategic Research Foundation at Private Universities (2011 to 2015).

Disclosures: None declared.

http://dx.doi.org/10.1016/j.ajpath.2014.02.006

interdigitated foot processes bridged by slit diaphragms, glomerular endothelial cells, and the intervening GBM[6] that these two cell types together produce.[7] Mesangial cells (MCs), the third cell type of the glomerulus, comprise approximately one-third of the glomerular tuft cell population. MCs bind the GBM at the base of the glomerular capillary loops to establish and maintain the structural architecture of the glomerular capillaries,[6] similar to the function of certain microvascular pericytes. These cells also contribute to mesangial matrix homeostasis, regulate filtration surface area and capillary blood pressure, and phagocytose apoptotic cells and immune complexes formed at or delivered to the glomerular capillaries. Cell biological and biochemical studies have characterized MC responses to hormones, cytokines, growth factors, and metabolic, inflammatory, and immune mediators that are highly relevant to primary glomerular diseases or to systemic diseases that target glomerular cells.[8]

Because inactivation of the *Lama1* gene in mice results in a failure of assembly of Reichert's membrane and developmental arrest shortly after implantation,[9] *in vivo* studies of LAMA1 function have been limited. Herein, we used a conditional *Lama1* knockout (KO) mouse model ($Lama1^{CKO}$) with specific deletion of *Lama1* in the epiblast lineage using *Sox2-Cre* to study the role of LAMA1 in kidney development and function. We found that the absence of LAMA1 delayed glomerular development, and adult $Lama1^{CKO}$ mice developed focal glomerulosclerosis and proteinuria with age. MCs from $Lama1^{CKO}$ mice showed increased proliferation, resulting in expansion of the mesangial cell compartment. Thus, LAMA1 plays a critical role in MC homeostasis and kidney function.

Materials and Methods

Animal Experiments

Conventional *Lama1* KO ($Lama1^{del/del}$) mice die at approximately embryonic day 7 because of lack of Reichert's membrane.[9,10] In a previous study, floxed *Lama1* ($Lama1^{flox/flox}$) mice and heterozygous *Lama1* null mice carrying the *Sox2-Cre* transgene ($Lama1^{del/+}$; $Sox2\text{-}Cre^{cre/+}$) were generated.[11] $Lama1^{CKO}$ ($Lama1^{floxed/del}$; $Sox2\text{-}Cre^{cre/+}$) mice with a conditional *Lama1* deficiency, specifically in the epiblast, and its derivatives, which comprise the entire embryo, were then generated by crossing the two lines. Genotypes were confirmed by PCR of tail-snip DNA.[11] Animals examined included male and female mice, aged 1 day to 24 months. $Lama1^{flox/flox}$ [wild-type (WT)] mice and $Lama1^{flox/del}$ (heterozygous) mice were used as normal controls.

Immunofluorescence

Kidneys from 7-month-old mice were fixed with 4% PFA in 0.1 mol/L PBS, pH 7.4, overnight at 4°C and then cryoprotected in 30% sucrose in PBS for 72 hours at 4°C. Sections (4 μm thick) were cut with a cryostat and mounted onto glass slides. For immunostaining, the frozen sections were air dried and washed with PBS. The sections were incubated with 0.1% Triton X-100 (Polysciences, Inc., Warrington, UK) in PBS for 15 minutes. After washing, they were blocked with blocking buffer (5% normal donkey serum and 2% bovine serum albumin in PBS) for 30 minutes and incubated with dilutions of the primary antibody in the blocking buffer for 1 hour. The following primary antibodies were used: rabbit anti-laminin α1 (LAMA1)[12]; rabbit anti-laminin α2 (LAMA2), rabbit anti-laminin α3 (LAMA3), rabbit anti-laminin α4 (LAMA4), and rabbit anti-laminin α5 (LAMA5) (gifts from Dr. Takako Sasaki); rat anti-laminin γ1 (LAMC1) (Chemicon International, Inc., Temecula, CA); mouse anti-synaptopodin (Progen Biotechnik, Heidelberg, Germany); rat anti-platelet endothelial cell adhesion molecule (PECAM; BD Pharmingen, Erembodegem, Belgium); and rabbit anti-smooth muscle actin (Abcam, Cambridge, MA). The slides were washed with PBS and incubated with the secondary antibodies, Alexa 488 donkey anti-rabbit (Molecular Probes, Eugene, OR), Cy3 donkey anti-mouse, and Cy 5—conjugated donkey anti-rat (Jackson ImmunoResearch Laboratories, Baltimore, MD) for 1 hour. In each experiment, several sections were incubated without the primary antibody to serve as controls. When the primary antibody was omitted from the staining, no immunoreactivity was observed.

Histological and Morphometric Data

For histological data, mice were perfused with 4% paraformaldehyde (PFA) under anesthesia. Kidney pieces from 2- to 24-month-old mice were fixed in 4% PFA and embedded in paraffin. Sections (4 μm thick) were deparaffinized with xylene, hydrated in a graded series of ethanol, and washed with PBS.

For morphometric analysis of glomeruli, sections were stained with either PAS or toluidine blue. Mesangial area was quantified by a blind observer (L.N.). Fifteen glomeruli cut at the vascular pole were randomly selected in PAS-stained sections from each animal in each experimental group. The increase in mesangial matrix (defined as mesangial area) was determined by the presence of PAS-positive and nuclei-free areas in the mesangium; the glomerular area was also traced along the outline of capillary loops using Imaging System KS400 (Imaging Associates, Thame, UK).

For electron microscopy, small pieces of kidney cortex from neonatal and 2- to 16-month-old mice were fixed in 2.5% glutaraldehyde in PBS. Tissues were dehydrated and embedded in plastic, and ultrathin sections were viewed by transmission electron microscopy, as previously described.[13] GBM thickness at 15 months of age in three $Lama1^{CKO}$ mice and three heterozygous mice was determined by using the orthogonal intercept method.[14] The degree of foot process effacement was evaluated by foot process width. A foot process was defined as any connected epithelial segment butting on the basement membrane between two neighboring filtration pores or slits. From each image, the

arithmetic mean of the foot process width was calculated, as described previously,[15] using the following equation:

$$\pi/4 \times \sum \text{GBM length} \Big/ \sum \text{foot process.} \quad (1)$$

where $\sum$ foot process is the total number of foot processes counted in each image, $\sum$ GBM length is the total GBM length measured in each image, and the correction factor of $\pi/4$ serves to correct for presumed random variation in the angle of section relative to the long axis of the podocyte.

Urine Albumin and Creatinine Assays

At monthly intervals beginning at 4 months of age, mice were placed in metabolic cages, and urine was collected for 24 hours. In some cases, 10 μL of urine in loading buffer was analyzed on SDS-PAGE gels stained with Coomassie Brilliant Blue. The urinary albumin-creatinine ratio was determined by immunoassay (DCA Vantage Analyzer; Siemens Healthcare Diagnostics, Deerfield, IL).

Cell Culture

Glomeruli were isolated through the injection of magnetic beads, which become trapped within glomerular capillaries.[16] Briefly, anesthetized 2-month-old mice were perfused with 8×10^7 Dynabeads M-450 (Invitrogen, Carlsbad, CA). The kidneys were removed and minced on ice, followed by digestion at 37°C with 1 mg/mL collagenase and 100 U/mL DNase I for 30 minutes, then filtered twice with 100-μm Falcon cell strainers (BD Falcon, Bedford, MA). The tissue was pelleted by gentle centrifugation (200 × *g*, 5 minutes), and glomeruli containing Dynabeads were collected using a magnetic particle concentrator (Dynal, Oslo, Norway) and washed in HBSS three times. Isolated glomeruli were cultured on type I collagen-coated culture dishes (BD BIOCOAT, Bedford, MA) in Dulbecco's modified Eagle's medium supplemented with 20% heat-inactivated fetal bovine serum, 100 μg/mL streptomycin, and 100 U/mL penicillin at 37°C in a humidified 95%/5% air/CO_2 atmosphere. When primary glomerular explant cultures reached day 30, cells were washed with PBS and removed from dishes by trypsinization (0.05% trypsin). Cells at passage 5 to 8 were characterized and used for the experiments. MCs cultured on chamber slides were fixed in 4% PFA and processed for immunofluorescence microscopy using antibodies for podocytes, endothelial cells, and MCs, as described previously.[17]

Analysis of Cell Proliferation

MCs were seeded in 8-well chamber slides (5×10^3 cells per well) and cultured with or without 5 μg/mL LM-111, LM-211, or LM-511 (Biolamina, Sundbyberg, Sweden). After 48 hours of culture, cell proliferation was assessed by measuring the incorporation of 5-bromo-2′-deoxyuridine (BrdU) into cellular DNA by an immunofluorescence assay (Kit 1-1296736; Roche, East Sussex, UK). Cells were incubated with 10 μmol/L BrdU (final concentration) for 60 minutes before fixation. The number of BrdU-positive cells was counted and expressed as a percentage of the total number of cells counted per field. At least five separate fields per well were examined. A negative control in which the anti-BrdU primary antibody was omitted was also assayed in each trial.

RT-PCR and Real-Time PCR Analysis

Total RNA was extracted from the MCs with TRIzol reagent, according to the manufacturer's instructions (Invitrogen). cDNA was synthesized from 2 μg of total RNA using oligo dT primers (Invitrogen) and Superscript III Reverse Transcriptase (Invitrogen). Real-time quantitative PCR (qPCR) was performed using SYBR Green PCR Master MIX and an ABI Prism 7500 Fast Sequence Detection System (Applied Biosystems, Santa Clara, CA). The primers used for transforming growth factor (TGF)-β1, glyceraldehyde-3-phosphate dehydrogenase (GAPDH) amplification were as follows: TGF-β1 5′-ACCTTGGTAACCGGCTGC-3′ (forward) and 5′-TCCTTGGTTCAGCCACTGC-3′ (reverse); and GAPDH 5′-ACGGCAAATTCAACGGCACAG-3′ (forward) and 5′-AGACTCCACGACATACTCAGCAC-3′ (reverse). Each sample was run in triplicate and normalized to GAPDH expression.

ELISA Data

A sample of 1 N HCl (20 μL) was added to 100 μL of cell culture supernatant and incubated for 10 minutes to activate latent TGF-β1. After the supernatants were neutralized with 1.2 N NaOH/0.5 mol/L HEPES, the samples were analyzed with a commercial TGF-β1 sandwich enzyme-linked immunosorbent assay (ELISA; R&D Systems, Minneapolis, MN), according to the manufacturer's recommendations. A standard curve was constructed using serial dilutions of ultrapure human TGF-β1 (R&D Systems). The amount of secreted TGF-β1 was normalized using total cellular proteins. Each sample was measured in duplicate.

Western Blot Analysis

MCs were seeded at a density of 3×10^5 cells per dish, grown to 70% confluence, and cultured in the absence or presence of 5 μg/mL LM-111 for 24 hours. After serum starvation for 24 hours in the absence or presence of 5 μg/mL LM-111, cells were treated with 10 ng/mL TGF-β1 (WAKO, Osaka, Japan) for 30 minutes. To study the effect of TGF-β1 receptor I (TβRI) kinase inhibitors on Smad2 phosphorylation, cells were serum starved and treated with increasing concentrations of SB-431542 (0.1, 1, 5, and 10 μmol/L) or dimethyl sulfoxide (Sigma-Aldrich, St. Louis, MO) in the presence of 10 ng/mL TGF-β1 for 30 minutes.[18] Protein extracts were prepared in lysis buffer (Cell Signaling, Danvers, MA) containing 1 mmol/L phenylmethylsulfonyl fluoride, 10 mmol/L

Na_3VO_4, and 2 mmol/L NaF, as well as phosphatase inhibitor cocktail. After incubation at 4°C for 30 minutes, nuclear and cellular debris were removed by centrifugation at 20,000 × *g* for 15 minutes at 4°C. Protein was quantified by BCA assay (Thermo Scientific, Rockford, IL) and 10 μg of protein per lane was separated by SDS-PAGE. Western blot analysis was performed as described previously.[19] The primary antibody used was anti−phospho-Smad2 (Ser465/467) (1:1000; Cell Signaling). The blots were subsequently reprobed with anti-Smad2/3 (1:1000; Cell Signaling). For the TβRI and collagen IV (COLIV) expression analysis, primary antibodies for TβRI (1:1000; Abcam) and COLIV (1:1000; Abcam) were used. The blots were subsequently reprobed with anti−β-actin antibody (1:1000; Santa Cruz Biotechnology, Inc., Santa Cruz, CA). Horseradish peroxidase−labeled secondary antibody to rabbit IgG or mouse IgG (1:1000) was purchased from GE Healthcare (Piscataway, NJ). Super Signal West Dura Extended Duration Substrate (Thermo Scientific) was used for detection of signals, and the images were captured using LAS-3000 mini (Fujifilm, Tokyo, Japan). Densitometry analysis of band intensity was performed using Multi Gauge version 3.0 (Fujifilm).

Transfection

FuGENE HD (Promega, Madison, WI) was used for transfection. Mesangial cells were plated on 6-well plates, grown to 50% to 60% confluence, and then transfected with either pcDNA3.1-*Lama1* or control pcDNA3.1. FuGENE HD Transfection Reagent (3 μL) was added to the DNA solution (1 μg in 100 μL Optimem). The mixture was incubated for 15 minutes at room temperature, then added to the cells. The cells were treated with TGF-β1 for 24 hours after transfection.

Statistical Analysis

Data are expressed as means ± SEM. A two-sided Student's *t*-test was used for comparisons between two groups. $P < 0.05$ was considered statistically significant.

Results

Delayed Kidney Development in Lama1-Deficient (*Lama1*^{CKO}) Mice

LAMA1 has been implicated in kidney development on the basis of results from organotypic cultures.[20,21] However, the *in vivo* function of LAMA1 in kidney is unknown, primarily because *Lama1* KO mice die at early embryonic stages. Herein, we used a viable conditional KO mouse (*Lama1*^{CKO}) model with a Sox2-Cre−mediated deletion of *Lama1* specifically in the epiblast lineage, which produces all embryonic tissues.[22] This enabled us to study the role of LAMA1 in kidney development and function. We first examined developing nephrons in newborn *Lama1*^{CKO} mice because all stages of nephrogenesis can be visualized in the newborn cortex.[22] We observed all appropriate developmental stages in both control and *Lama1*^{CKO} mice, including mesenchymal condensates and comma-shaped bodies (data not shown), S-shaped bodies (Figure 1, A and D), capillary loop stages with forming glomerular capillaries (Figure 1, B and E), and maturing glomeruli with blood cells in the capillaries (Figure 1, C and F). We next quantitated the extent of nephron/glomerular development for each developmental stage in control and *Lama1*^{CKO} mice as percentages of the total (Figure 1G). The percentage of maturing and fully mature glomeruli was significantly decreased in *Lama1*^{CKO} mice compared with controls. These results showed that glomerular development was delayed in *Lama1*^{CKO} mice. To investigate whether the delay in glomerular development caused fewer nephrons in *Lama1*^{CKO} mice, we measured numbers of glomeruli in *Lama1*^{CKO} and control kidneys from 2-month-old mice. We found that there was no significant difference in numbers of glomeruli between control and *Lama1*^{CKO} mice (Figure 1H).

Renal Abnormalities in Adult *Lama1*^{CKO} Mice

Laminin isoform composition differs in GBM and in the mesangial matrix, and it changes with glomerular development.[5,23] In some renal diseases, the normal transition and final composition are altered.[22,24−28] Immunostaining revealed that, in *Lama1*^{CKO} mice, LAMA1 was absent from the mesangium (Figure 2B), whereas it was expressed in control mice (Figure 2A), as shown previously.[5] LAMA2 was detected in the mesangium at a higher level in mutant versus control (Figure 2, C and D), and LAMA4 was also detected weakly in glomeruli of both control and *Lama1*^{CKO} mice (Figure 2, E and F). LAMA5 was detected in virtually all GBM segments (Figure 2, G and H), in agreement with previous studies.[5] LAMC1 (γ1) was detected in both the GBM and the mesangium in control and in *Lama1*^{CKO} kidneys, but increased in the *Lama1*^{CKO} mesangium (Figure 2, I and J). These data show that even though LAMA1 was absent from glomeruli, the distribution of the other laminin α chains in glomeruli was similar to those of normal mice, except for stronger immunostaining for LAMA2 and LAMC1 in the mesangium of *Lama1*^{CKO} mice.

Increased levels of LAMA2 and LAMC1 (as well as perlecan; data not shown) in the mesangium indicated a possible expansion of the mesangial compartment in *Lama1*^{CKO} kidneys. Histological examination by light microscopy revealed abnormalities in *Lama1*^{CKO} mice compared with the control exclusively in glomeruli. In agreement with the immunofluorescence, dividing kidneys into sections (9 heterozygous, 1 WT, and 11 *Lama1*^{CKO} females at 7 months), followed by PAS staining, showed mesangial expansion in *Lama1*^{CKO} mice (Figure 3, A−D). Mesangial expansion was quantitated by a morphometric analysis; the PAS-positive and nuclei-free mesangial area in the glomeruli of *Lama1*^{CKO} mice was 44% more than that in

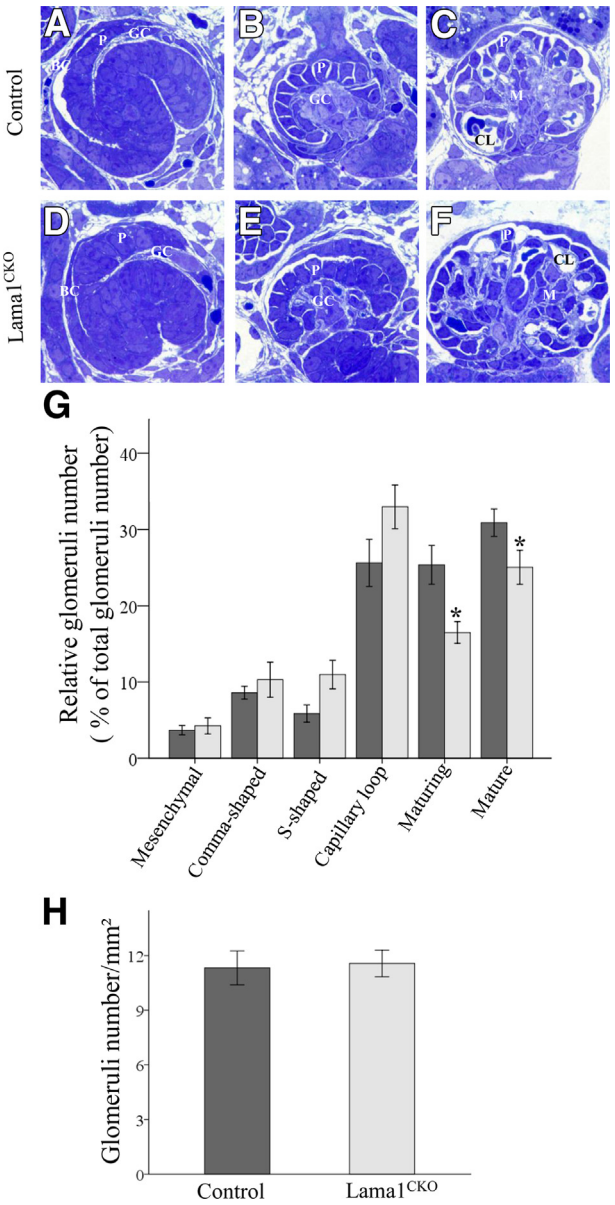

Figure 1 Histological characteristics of glomerular development. **A**—**F:** Toluidine blue—stained sections from newborn (post-natal day 1) mouse kidneys. **A** and **D:** S-shaped body. A capillary loop is present in the cleft. **B** and **E:** Capillary loop stage glomeruli showing the cup-shaped arrangement of the podocytes. **C** and **F:** Mature glomeruli. The percentage of glomeruli at each developmental stage in control and *Lama1*^{CKO} mice. **G:** Significantly lower percentages of maturing and mature glomeruli are observed in *Lama1*^{CKO} kidneys (light gray bars) compared with the controls (dark gray bars). **H:** There is no significant difference in the number of glomeruli observed in *Lama1*^{CKO} versus control kidneys at 2 months of age. Data represent means ± SEM. *$P < 0.05$ versus control at same glomerular developmental stage. Original magnification, ×1000 (**A**—**F**). BC, Bowman's capsule; CL, capillary loop; GC, glomerular cleft; M, mesangial cells; P, podocyte progenitors.

control mice (Figure 3E). Total glomerular area was defined by tracing along the outline of the capillary loops and was decreased in *Lama1*^{CKO} mice compared with control mice (Figure 3F). Thus, the relative mesangial area, as calculated by determining the mesangial area/total glomerular area ratio, was increased by 67% in the *Lama1*^{CKO} mice (Figure 3G).

Taken together, these findings indicate that LAMA1 plays a role in mesangial cell homeostasis and that other laminin α chains cannot substitute for Lama1 in mediating this function.

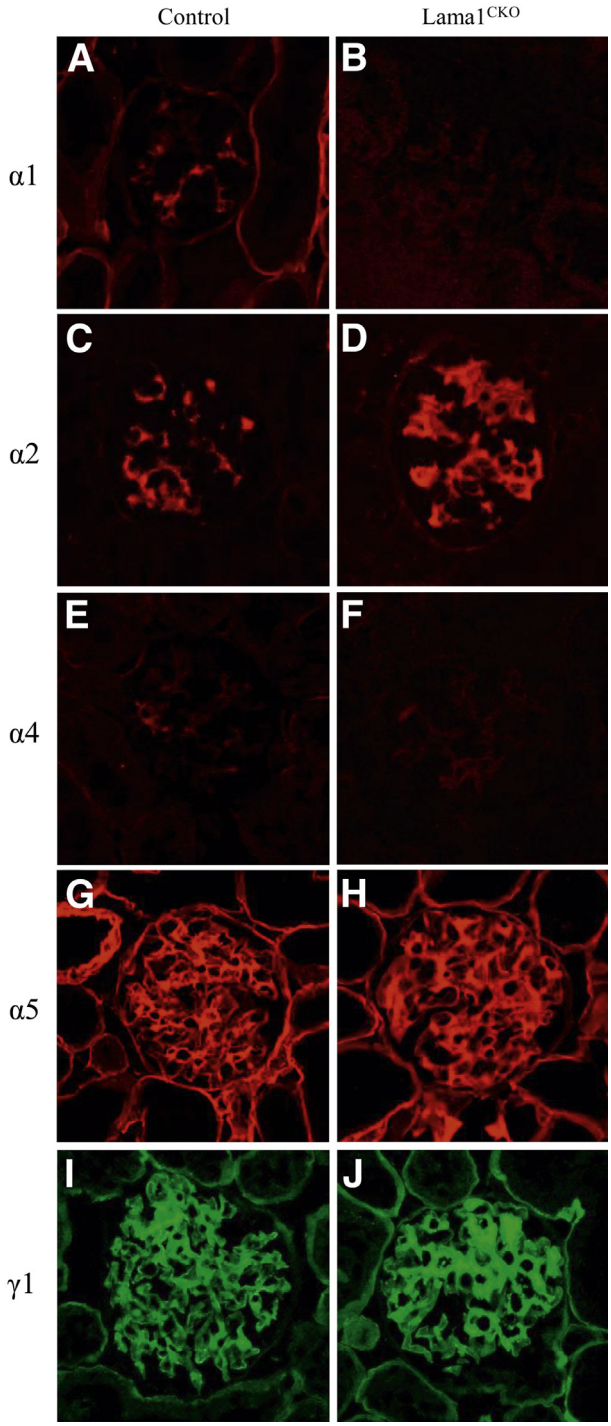

Figure 2 Immunofluorescence microscopic analysis of laminin chain deposition. Basement membranes and mesangial matrix were stained with anti-laminin α1, α2, α4, and α5 (red), and anti-laminin γ1 (green) antibodies, as indicated. LMα1 is detected in the mesangial matrix in control mice (**A**) and is absent in *Lama1*^{CKO} mice (**B**). There are no detectable differences in laminin α chain immunolocalization (**C**—**J**), but LMα2 and LMγ1 increase in the mesangial matrix in *Lama1*^{CKO} mice (**D** and **J**). Original magnification, ×400 (**A**—**J**).

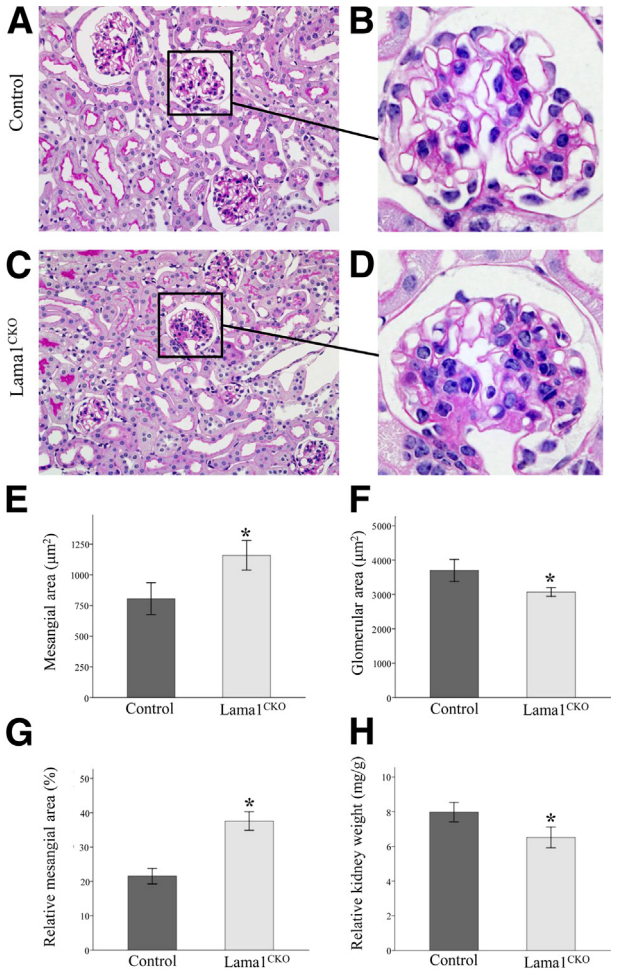

Figure 3 Light microscopy reveals renal abnormalities in adult *Lama1*^{CKO} mice. **A**–**D:** Representative images of PAS-stained kidney specimens from 6- to 8-month-old control and *Lama1*^{CKO} mice. **C** and **D:** Glomerular size reduction and mesangial expansion are observed in *Lama1*^{CKO} mice. The graphs depict quantitative measurements of mesangial area (**E**), glomerular area (**F**), and relative mesangial matrix area (**G**) of control (dark gray bars) versus *Lama1*^{CKO} (light gray bars) mice. **H:** The average kidney weight relative to total body weight is shown. Data represent means ± SEM. **P* < 0.05 versus control. Original magnifications: ×400 (**A** and **C**); ×1000 (**B** and **D**).

In addition to the abnormalities in the mesangium, a significant difference in kidney weight between *Lama1*^{CKO} mice and control mice was observed, with the kidney weight of *Lama1*^{CKO} mice being lower than that of controls at 7 months of age (data not shown). These differences remained significant when values were normalized to body weight (Figure 3H).

Lama1^{CKO} Mice Develop Glomerulosclerosis with Increased MC Proliferation and Mesangial Matrix Expansion with Age

We next examined aging-associated glomerular pathological features in *Lama1*^{CKO} mice at 2 to 24 months of age. Before 6 months of age, no significant renal histopathological changes were observed in either control or *Lama1*^{CKO} mice (data not shown). However, after 6 months of age, *Lama1*^{CKO} mice showed mesangial cell proliferation and mesangial matrix expansion compared with control mice (Figure 4, D–F and J–L). As *Lama1*^{CKO} mice aged further, mesangial cell numbers stayed the same, but mesangial matrix expansion increased (Figure 4, M and N). By 6 to 8 months of age, *Lama1*^{CKO} mice showed a moderate mesangial matrix

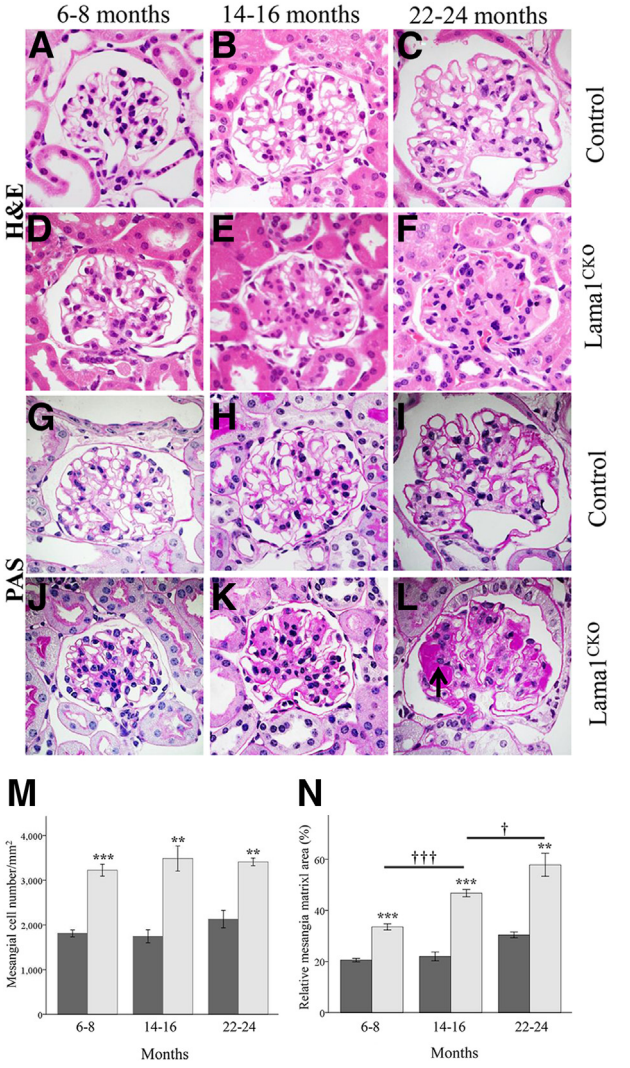

Figure 4 Light microscopy reveals progressive development of glomerulosclerosis in *Lama1*^{CKO} mice. Representative micrographs of PAS- and H&E-stained glomeruli in control and *Lama1*^{CKO} mice aged 7, 15, and 23 months (as indicated). H&E staining shows matrix expansion in the *Lama1*^{CKO} mouse (**D**–**F**) compared with the control (**A**–**C**). **E:** At 14 to 16 months, the *Lama1*^{CKO} mice showed moderate mesangial sclerosis. **F:** As the *Lama1*^{CKO} mice aged, mesangial sclerosis became more conspicuous. PAS staining revealed increased mesangial cell proliferation and GBM thickening in the *Lama1*^{CKO} (**J**–**L**) compared with the control (**G**–**I**) mice. **L:** PAS^{+} nodular mesangial sclerosis was observed in *Lama1*^{CKO} mice at 22 to 24 months of age (**arrow**). **M** and **N:** Quantitative measurements of mesangial cell number and relative mesangial matrix area (per total glomerular tuft cross-sectional area) for control (dark gray bars) and *Lama1*^{CKO} (light gray bars) mice. Data represent means ± SEM. ***P* < 0.01, ****P* < 0.001 versus control at same age; $^{\dagger}P$ < 0.05 versus 14- to 16-month-old mice; $^{\dagger\dagger\dagger}P$ < 0.001 versus 6- to 8-month-old mice. Original magnification, ×1000 (**A**–**L**).

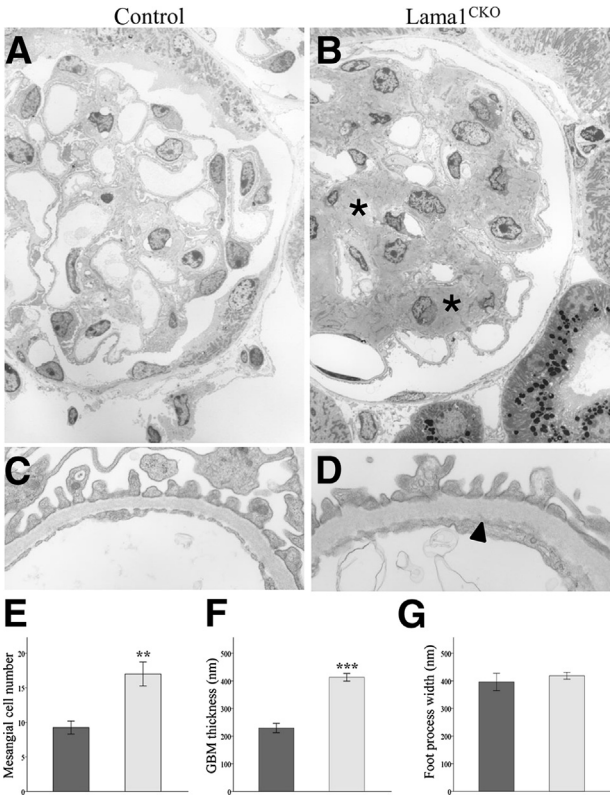

Figure 5 Electron microscopic analysis of glomeruli. Representative electron micrographs of control (**A** and **C**) and *Lama1*^{CKO} (**B** and **D**) glomeruli at 14 to 16 months of age. *Lama1*^{CKO} mice had significant mesangial expansion (**asterisks**) and GBM thickening (**arrowhead**). **E**–**G:** Quantitation of the indicated features in control (dark gray bars) and *Lama1*^{CKO} (light gray bars) mice show significant increases in mesangial cell number and GBM thickness but no significant difference was observed in podocyte foot process width. Data represent means ± SEM. $^{**}P < 0.01$, $^{***}P < 0.001$ versus control. Original magnifications: ×1000 (**A** and **B**); ×10,000 (**C** and **D**).

expansion, but they did not exhibit glomerulosclerosis (Figure 4, D and J). By 14 to 16 months of age, 35% of *Lama1*^{CKO} mice showed numerous segmentally sclerosed glomeruli (Figure 4E) associated with GBM thickening (Figure 4K), whereas no control mice showed glomerulosclerosis with GBM thickening (Figure 4, B and H). By 22 to 24 months of age, most Lama1^{CKO} mice had many globally and segmentally sclerosed glomeruli (Figure 4, F and L), and PAS^{+} nodular mesangial sclerosis was observed (Figure 4L). Control mice also showed moderate mesangial expansion and GBM thickening at this age, but only rarely showed glomerulosclerosis (Figure 4, C and I). Glomerular abnormalities were characterized in more detail by electron microscopy in mice aged 14 to 16 months (Figure 5). In agreement with light microscopy, there were more MCs and an increased amount of mesangial matrix in old *Lama1*^{CKO} mice compared with controls (Figure 5B). Many areas of GBM thickening were also observed (Figure 5D). These data show that older *Lama1*^{CKO} mice exhibit a greater degree of MC and matrix irregularities versus controls, presumably associated with aging.

Defects in Renal Function of *Lama1*^{CKO} Mice

Because glomerular structure can influence glomerular filtration,[6] the glomerular abnormalities in *Lama1*^{CKO} mice led us to look for alterations in renal function. Urine from *Lama1*^{CKO} and control mice was collected every 2 months and analyzed (Figure 6). Coomassie Blue staining of urine samples from *Lama1*^{CKO} mice showed an increased level of albumin compared with controls (Figure 6A). We also consistently detected higher urinary albumin/creatinine ratios in *Lama1*^{CKO} mice at 6 to 24 months of age, and the difference increased as the mice aged (Figure 6B). These results demonstrate a progressive defect in the kidney's ability to handle albumin in *Lama1*^{CKO} mice.

MCs from *Lama1*^{CKO} Mice Show Increased Proliferation *in Vitro*

In vivo studies have provided evidence that LAMA1 deficiency promotes MC proliferation. To investigate this further, we examined MC proliferation *in vitro*. Primary cultures derived from mouse glomeruli yielded a homogeneous population of MCs (Figure 7, A–C). These were characterized by their stellate/spindle-shaped morphological features, positive staining for α-smooth muscle actin, and negative staining for synaptopodin and PECAM, which are specific for podocytes and endothelial cells, respectively. MCs from *Lama1*^{CKO} mice exhibited significantly increased proliferation compared with those from control mice (Figure 7D).

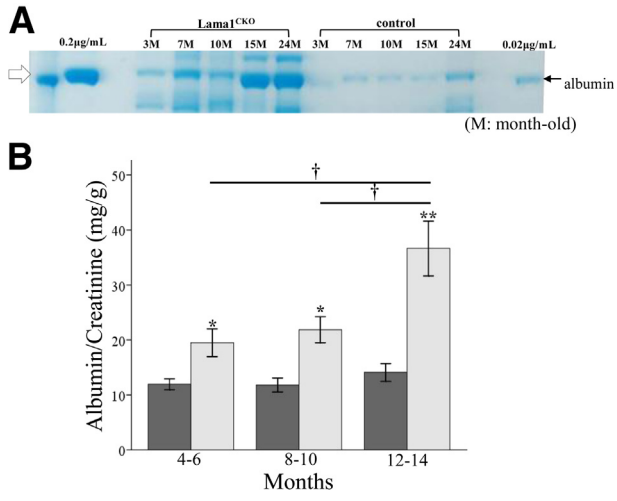

Figure 6 Analysis of renal function. **A:** Urine from 3- to 24-month-old (M) *Lama1*^{CKO} and control mice was collected and analyzed by SDS-PAGE and Coomassie Blue staining. The **arrow** denotes approximately 66 KDa, the size of excreted albumin. *Lama1*^{CKO} mice have a higher concentration of albumin as they age compared with control mice. **B:** Urine was collected for 24 hours from control (dark gray bars) and *Lama1*^{CKO} (light gray bars) mice and analyzed for albumin/creatinine ratio. Ratios in *Lama1*^{CKO} mice are higher than in controls. Data represent means ± SEM. $^{*}P < 0.05$, $^{**}P < 0.01$ versus control; $^{\dagger}P < 0.05$ versus 4- to 6-month-old mice and 8- to 10-month-old mice.

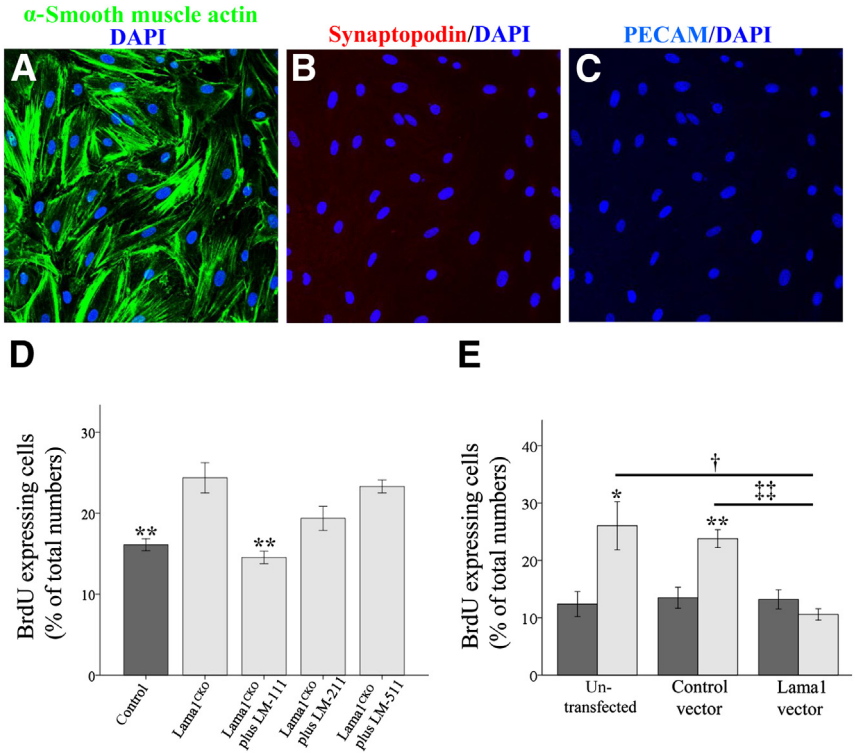

Figure 7 Analysis of primary mesangial cells. Mesangial cells are elongated, arranged in multiple layers, and stained positively for smooth muscle α-actin (**A**), but not synaptopodin (**B**) or PECAM (**C**). **D:** Proliferation was assessed by immunofluorescence assay for BrdU-positive cells as a percentage of the total number of cells, averaged from five separate fields of view. Mesangial cells from *Lama1*^{CKO} mice exhibit significantly increased proliferation compared with control cells. This increase is inhibited by exogenous LAMA1-containing LM-111, but not by LAMA2- or LAMA5-containing isoforms. **E:** Mesangial cell proliferation determined in cells transfected with vector alone or with a LAMA1 expression vector. Control (dark gray bars) and *Lama1*^{CKO} (light gray bars) cells were cultured on slide chambers for 24 hours and transfected for 48 hours before proliferation analysis. Restoration of LAMA1 expression by *Lama1*^{CKO} cells suppresses their proliferation. Data represent means ± SEM. $^{*}P < 0.05$, $^{**}P < 0.01$ versus control; $^{\dagger}P < 0.05$ versus untransfected cells; $^{\ddagger\ddagger}P < 0.01$ versus control vector transfected cells.

After this, we tested MC proliferation by treatment with LM-111, LM-211, or LM-511. The increase in MC proliferation was inhibited by exogenous LM-111, but not by either LM-211 or LM-511 (Figure 7D). We also tested whether LAMA1 deficiency is directly involved in this increased MC proliferation by transfection of *Lama1*^{CKO} MCs with a *Lama1* expression vector. RT-qPCR analysis showed the expression of *Lama1* mRNA in *Lama1*^{CKO} MCs transfected with the *Lama1* vector (Supplemental Figure S1B). We found that the expression of exogenous *Lama1* abrogated the increased proliferation of *Lama1*^{CKO} MCs, whereas the control empty vector did not (Figure 7E), suggesting that LAMA1/LM-111 plays a specific role in regulating MC homeostasis.

Loss of LAMA1 Increases TGF-β/Smad Signaling in *Lama1*^{CKO} MCs

TGF-β/Smad signaling is a major pathway involved in renal fibrosis.[29] Binding of TGF-β1 to TβRII activates TβRI kinase, which phosphorylates Smad2 and Smad3. The phosphorylated Smad2 (p-Smad2) and p-Smad3 then bind to Smad4 and form the Smad complex, which translocates into the nucleus and regulates target gene transcription.[29] Smad7 is an inhibitory Smad that blocks TGF-β–induced Smad-dependent fibrosis. Because TGF-β1 stimulates the synthesis and inhibits the degradation of extracellular matrix molecules,[30] and is associated with increased mesangial matrix in several glomerular diseases,[30–32] we investigated the effect of the absence of LAMA1 on TGF-β signaling. We first examined the level of TGF-β1 mRNA and protein secreted in *Lama1*^{CKO} MCs. We did not detect significant differences compared with control MCs (Figure 8, A–C), indicating that the absence of LAMA1 does not alter the levels of TGF-β1 expression. Next, we examined the levels of p-Smad2 in the absence of LAMA1. The addition of TGF-β1 increased p-Smad2 levels to a greater extent in *Lama1*^{CKO} cells than in control cells (Figure 8D), suggesting that the absence of LAMA1 increases TGF-β/Smad signaling. The basal phosphorylation level of Smad2 in *Lama1*^{CKO} MCs was higher than that in control MCs (Supplemental Figure S2) when cells were cultured without serum starvation. In addition, LM-111 treatment rescued the increased TGF-β1–induced Smad2 phosphorylation in *Lama1*^{CKO} cells, implying that LAMA1 likely plays a direct role in dampening the levels of TGF-β1–mediated Smad2 phosphorylation in MCs. Furthermore, we sought to elucidate the mechanism of increased Smad2 phosphorylation in the absence of LAMA1. MCs were pretreated with SB431542, a specific and potent inhibitor of TGF-β–induced phosphorylation of Smad2 by TβRI.[33] SB431542 was added to the control and *Lama1*^{CKO} cells at varying doses, and cells were treated for 30 minutes with TGF-β1. Cell lysates were collected and processed for Western blot analysis of p-Smad2 levels. Decreased or loss of Smad2 phosphorylation was observed in a dose-dependent manner for both control and *Lama1*^{CKO} cells (Figure 8E). These data show that all of the phosphorylation of Smad2 occurs via the activity of TβRI, regardless of the presence or absence of LAMA1. This indicates that LAMA1 plays a direct role in limiting TGF-β/Smad

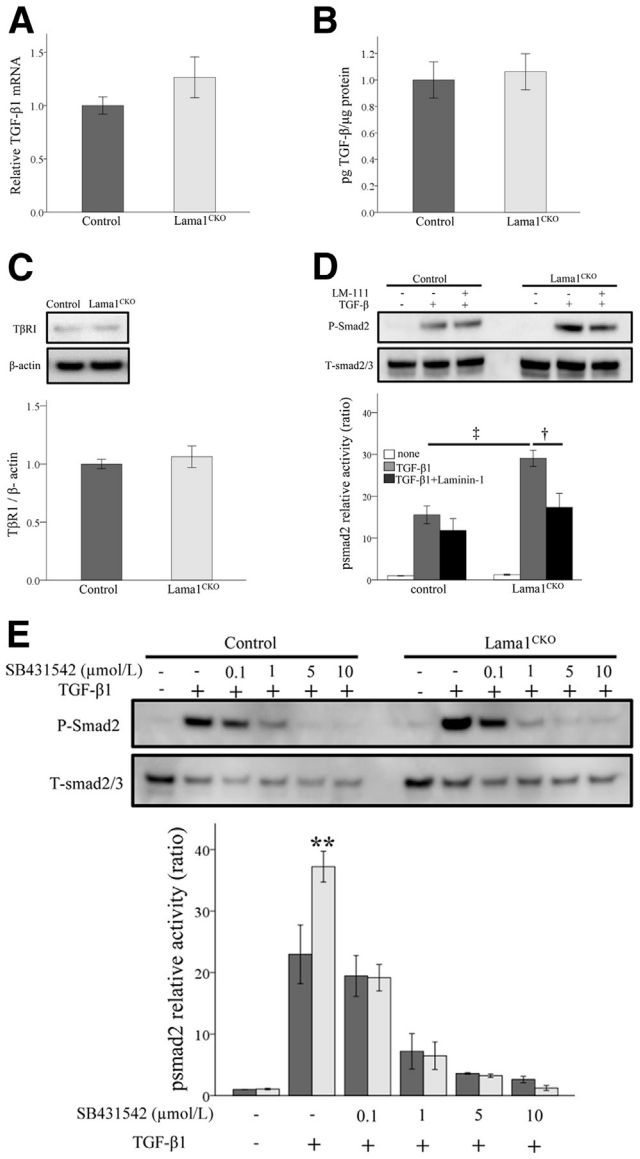

Figure 8 TGF-β1/Smad signaling in mesangial cells from *Lama1*^{CKO} and control mice. **A** and **B:** TGF-β1 mRNA expression and secretion in mesangial cells. MCs were cultured for 48 hours and serum starved for an additional 48 hours before total mRNA extraction and culture media collection. **A:** TGF-β1 mRNA expression levels measured by RT-qPCR. The bar graph represents the ratio between the TGF-β1 and GAPDH levels. **B:** Immunoreactive TGF-β1 synthesis measured by ELISA. **C:** Western blot analysis of TβRI protein levels in MCs. **D** and **E:** Smad2 phosphorylation determined by using Western blot analysis. The intensity of signal was analyzed by Multi Gauge version 3.0 (Fujifilm). Relative activity, expressed as the ratio of activated phospho-Smad2/total Smad2/3, was quantified as the fold increase relative to non-stimulation conditions (defined as 1). MCs from control and *Lama1*^{CKO} mice were cultured in the absence or presence of 5 μg/mL LM-111 for 24 hours. **D:** After serum starvation for 24 hours, cells were treated with 10 ng/mL TGF-β1 (WAKO) for 30 minutes. MCs from control and *Lama1*^{CKO} mice were serum starved for 24 hours, followed by 1-hour treatment with increasing concentrations of SB-431542 (0.1, 1, 5, and 10 μmol/L) or dimethyl sulfoxide (DMSO), and then stimulated for 30 minutes with 10 ng/mL TGF-β. **E:** Loss of Smad2 phosphorylation is observed in an SB-431542 dose-dependent manner for both control (dark gray bars) and *Lama1*^{CKO} (light gray bars) cells. Data represent means ± SEM. $^{**}P < 0.01$ versus control; $^{\dagger}P < 0.05$ versus laminin-1 treatment cells; $^{\ddagger}P < 0.01$ versus control cells.

signaling. Finally, because reduced Smad7 results in enhanced activation of TGF-β signaling,[34] we also investigated Smad7 expression in MCs. There was no significant difference in the level of Smad7 protein in control and in *Lama1*^{CKO} cells (data not shown).

TGF-β1—Induced Type IV Collagen Expression Is Increased in the Absence of LAMA1

Because *Lama1*^{CKO} mice showed a thickened GBM (Figure 5D), we examined the expression of COLIV, one of the major mesangial matrix components.[35] Immunostaining analysis revealed more COLIV deposition in the mesangium of *Lama1*^{CKO} mice than of control mice (Figure 9A). Previous studies have shown that TGF-β1 induces COLIV expression in mouse MCs.[36] Therefore, we examined the effect of TGF-β1 on COLIV expression in MCs prepared from *Lama1*^{CKO} mice. We found that TGF-β1 induced COLIV expression in both control and *Lama1*^{CKO} MCs, but the level of COLIV expression was significantly higher in *Lama1*^{CKO} MCs than in control cells (Figure 9, B and C). This higher COLIV expression level in *Lama1*^{CKO} MCs was abrogated by transfection with the LAMA1 expression vector, but not by transfection with the empty control vector (Figure 9D). These results suggest that LAMA1 is involved in the regulation of mesangial matrix production.

Discussion

Our interest in LM-111 function in the kidney was initially stimulated by the observation that *Lama1* has a rather restricted expression pattern. LAMA1 is found transiently in the developing GBM, is absent in the mature GBM, and is present in the glomerular mesangium in adult mice.[5] Herein, we demonstrated that Lama1 is critical for mesangial homeostasis and kidney function.

An impediment to elucidating kidney LAMA1 function had been that *Lama1* disruption results in lethality at an early embryonic stage.[1] We previously described the generation of a conditional KO of *Lama1* with selective deletion only in embryonic cells, wherein the early embryonic death observed in total *Lama1* KO mice was overcome. Our results demonstrate important functional roles for LAMA1, which are exemplified by delayed glomerular development, abnormal renal histological features, and impaired renal function. Increased MC proliferation and mesangial matrix expansion are remarkable features observed in *Lama1*^{CKO} mice.

Diabetic nephropathy is histologically characterized by thickening of the GBM and mesangial expansion.[37–39] The earliest morphological change in diabetic nephropathy is mesangial expansion due to increased mesangial matrix deposition and a mild increase in mesangial cellularity, as well as hypertrophy of mesangial cells. The characteristic histological changes of diabetic nephropathy are diffuse and

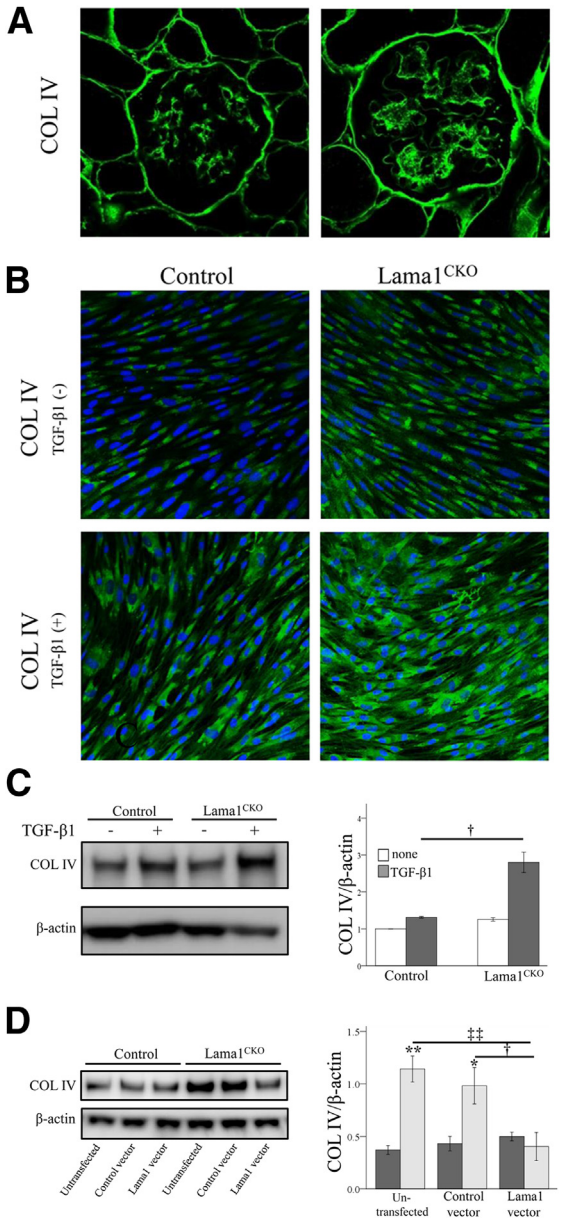

Figure 9 Expression of COLIV. **A:** The deposition of COLIV in the glomeruli of control and *Lama1*^{CKO} mice. Immunofluorescence staining for COLIV was performed in frozen tissue sections from 7-month-old mice. **B**–**D:** Effect of TGF-β1 on COLIV synthesis by MCs. Control and *Lama1*^{CKO} MCs were cultured on slide chambers for 24 hours, serum deprived for an additional 24 hours, and then treated with TGF-β1 for 24 hours. Immunofluorescence (**B**) and Western blot analysis (**C**) were performed to analyze COLIV synthesis and deposition. Values in **C** are expressed as COLIV/β-actin and quantified as the fold increase relative to control non-stimulation conditions (defined as 1). Control and *Lama1*^{CKO} MCs were cultured on 6-well plates for 24 hours and transfected for 48 hours before a 24-hour TGF-β1 treatment. $^{\dagger}P < 0.05$ versus TGF-β1 treatment control cells. **D:** COLIV protein levels were then determined by using Western blot analysis. β-Actin was used as a control. The intensity of signal was analyzed by Multi Gauge version 3.0 (Fujifilm). The absence of LAMA1 increases TGF-β1–induced COLIV expression. This increase was abrogated by transfection of *Lama1*^{CKO} (light gray bars) MCs with the LAMA1 expression vector; control MCs are represented by dark gray bars. $^{*}P < 0.05$, $^{**}P < 0.01$ versus control; $^{\dagger}P < 0.05$ versus control vector transfected cells; $^{\ddagger\ddagger}P < 0.01$ versus untransfected cells. Original magnification, ×400 (**A**).

nodular glomerulosclerosis, along with afferent and efferent hyaline arteriolosclerosis. A reduction in podocyte number is associated with foot process effacement.[40] In the present study, we observed GBM thickening, mesangial expansion, and increased mesangial cell proliferation from 6-month-old *Lama1*^{CKO} mice. As the mice aged, there was increased mesangial expansion due to glomerulosclerosis, which was accompanied by progressive proteinuria. These pathological conditions are similar to those seen in diabetic nephropathy, but we did not observe differences between *Lama1*^{CKO} and control mice in terms of podocyte number or foot process effacement. Although proteinuria was detectable in *Lama1*^{CKO} mice, this was at a lower level than in most kidney diseases. Because there is no or little LAMA1 in the GBM, podocytes would not be expected to have abnormalities. The proteinuria in the later stages was likely due to mesangial cell defects, which led to profibrotic cross talk that affected the podocytes, or perhaps due to some unknown mechanism.

Many studies have indicated that activated mesangial cells are the major cells responsible for the expression of interstitial matrix components, such as fibronectin and type I collagen, which directly result in mesangial expansion leading to glomerulosclerosis.[41] The present study demonstrated that the deletion of LAMA1 results in age-dependent mesangial expansion, which develops into focal glomerulosclerosis. These observations lead us to hypothesize that LAMA1 may be an endogenous negative regulator that specifically suppresses mesangial cell activation.

TGF-β is the most potent cytokine inducing mesangial cell activation both *in vitro* and *in vivo*.[42] It stimulates the expression of ECM proteins, including collagens, laminin, and fibronectin, while suppressing the synthesis of ECM protease inhibitors.[43] The Smad pathway is known to mediate the functions of TGF-β on renal fibrogenesis and subsequent ECM accumulation in diabetic nephropathy.[44] In the present study, we were unable to detect increased TGF-β1 mRNA expression in *Lama1*^{CKO} MCs. However, an alternative mechanism is suggested from the increased TGF-β1–induced Smad2 phosphorylation. In addition, inhibitors of TβRI kinase blocked Smad2 phosphorylation in both control and *Lama1*^{CKO} MCs. This supports the hypothesis that LAMA1 suppresses mesangial cell activation via inhibition of the TGF-β/Smad pathway.

Laminins not only function as structural components, but also bind cell surface receptors, including integrins and α-dystroglycan.[45] We demonstrated that LM-111 treatment abrogated the increased TGF-β1–induced Smad2 phosphorylation in *Lama1*^{CKO} cells. Furthermore, the restoration of LAMA1 expression in *Lama1*^{CKO} MCs by transfection with the LAMA1 expression vector inhibited the increased MC proliferation and TGF-β1–induced COLIV expression. We, therefore, speculate that LM-111 synthesized by WT mesangial cells inhibits TGF-β1 signaling. TGF-β1 signals through its type I and type II serine/threonine kinase receptors,[42] and this pathway is tightly controlled by multiple positive and negative regulator

proteins.[46] Negative regulation of TGF-β signaling is accomplished by the rapid attenuation or even inhibition of TβRI/II and/or Smad activities.[47,48] In extracellular compartments, decorin, a proteoglycan associated with matrix components, binds to active TGF-β1 and prevents it from engaging with its receptors.[49] In cell membranes, integrin signaling is involved in negatively regulating TGF-β signaling, because adhesion reduces TGF-β–induced Smad2 phosphorylation.[50] Laminins regulate cellular behavior through interactions with cell surface receptors, including integrins, syndecans, and α-dystroglycan.[1,51] In the cytoplasm, inhibitory Smad7 either competes with receptor-regulated Smad to bind to activated type I receptors or interacts with growth arrest and DNA damage protein, a regulatory subunit of the protein phosphatase 1 holoenzyme, which subsequently recruits catalytic subunit of PP1 to dephosphorylate and inactivate the TGF-β type I receptor.[52]

The present study demonstrated that excess Smad2 phosphorylation occurred in the absence of Lama1 via TβRI and the absence of LAMA1 did not change the expression of Smad7. In addition, the Biacore analysis and solid-phase binding assays showed that the active form of TGF-β bound to LM-111 (Supplemental Figure S3 and Supplemental Table S1). This suggests that LAMA1 may play a direct role in inhibiting TGF-β signaling by binding to active TGF-β1 to prevent it from engaging with its receptors or by interaction with integrin signaling, which is involved in negatively regulating TGF-β signaling.

Taken together, our results suggest that LAMA1 plays a role in negatively regulating TGF-β/Smad signaling. This may be important for maintaining mesangial cell populations and mesangial matrix deposition.

Acknowledgments

We thank Glenn Longenecker and Ashok B. Kulkarni for help generating mutant mice and Dr. Yasuo Uchiyama, Takashi Ueno, and Tsutomu Fujimura (Juntendo University, Tokyo, Japan) for useful advice.

Supplemental Data

Supplemental material for this article can be found at *http://dx.doi.org/10.1016/j.ajpath.2014.02.006*.

References

1. Miner JH, Yurchenco PD: Laminin functions in tissue morphogenesis. Annu Rev Cell Dev Biol 2004, 20:255–284
2. Aumailley M, Bruckner-Tuderman L, Carter WG, Deutzmann R, Edgar D, Ekblom P, Engel J, Engvall E, Hohenester E, Jones JC, Kleinman HK, Marinkovich MP, Martin GR, Mayer U, Meneguzzi G, Miner JH, Miyazaki K, Patarroyo M, Paulsson M, Quaranta V, Sanes JR, Sasaki T, Sekiguchi K, Sorokin LM, Talts JF, Tryggvason K, Uitto J, Virtanen I, von der Mark K, Wewer UM, Yamada Y, Yurchenco PD: A simplified laminin nomenclature. Matrix Biol 2005, 24:326–332
3. Ryan MC, Christiano AM, Engvall E, Wewer UM, Miner JH, Sanes JR, Burgeson RE: The functions of laminins: lessons from in vivo studies. Matrix Biol 1996, 15:369–381
4. Kleinman HK, Weeks BS, Schnaper HW, Kibbey MC, Yamamura K, Grant DS: The laminins: a family of basement membrane glycoproteins important in cell differentiation and tumor metastases. Vitam Horm 1993, 47:161–186
5. Miner JH, Patton BL, Lentz SI, Gilbert DJ, Snider WD, Jenkins NA, Copeland NG, Sanes JR: The laminin alpha chains: expression, developmental transitions, and chromosomal locations of alpha1-5, identification of heterotrimeric laminins 8-11, and cloning of a novel alpha3 isoform. J Cell Biol 1997, 137:685–701
6. Miner JH: Building the glomerulus: a matricentric view. J Am Soc Nephrol 2005, 16:857–861
7. Wang R, Moorer-Hickman D, St John PL, Abrahamson DR: Binding of injected laminin to developing kidney glomerular mesangial matrices and basement membranes in vivo. J Histochem Cytochem 1998, 46:291–300
8. Abboud HE: Mesangial cell biology. Exp Cell Res 2012, 318:979–985
9. Miner JH, Li C, Mudd JL, Go G, Sutherland AE: Compositional and structural requirements for laminin and basement membranes during mouse embryo implantation and gastrulation. Development 2004, 131:2247–2256
10. Alpy F, Jivkov I, Sorokin L, Klein A, Arnold C, Huss Y, Kedinger M, Simon-Assmann P, Lefebvre O: Generation of a conditionally null allele of the laminin alpha1 gene. Genesis 2005, 43:59–70
11. Ichikawa-Tomikawa N, Ogawa J, Douet V, Xu Z, Kamikubo Y, Sakurai T, Kohsaka S, Chiba H, Hattori N, Yamada Y, Arikawa-Hirasawa E: Laminin alpha1 is essential for mouse cerebellar development. Matrix Biol 2012, 31:17–28
12. Sasaki T: Expression and distribution of laminin α1 and α2 chains in embryonic and adult mouse tissues: an immunochemical approach. Exp Cell Res 2002, 275:185–199
13. Jarad G, Cunningham J, Shaw AS, Miner JH: Proteinuria precedes podocyte abnormalities in Lamb2-/- mice, implicating the glomerular basement membrane as an albumin barrier. J Clin Invest 2006, 116:2272–2279
14. Jensen EB, Gundersen HJ, Osterby R: Determination of membrane thickness distribution from orthogonal intercepts. J Microsc 1979, 115:19–33
15. Koop K, Eikmans M, Baelde HJ, Kawachi H, De Heer E, Paul LC, Bruijn JA: Expression of podocyte-associated molecules in acquired human kidney diseases. J Am Soc Nephrol 2003, 14:2063–2071
16. Takemoto M, Asker N, Gerhardt H, Lundkvist A, Johansson BR, Saito Y, Betsholtz C: A new method for large scale isolation of kidney glomeruli from mice. Am J Pathol 2002, 161:799–805
17. Yaoita E, Kurihara H, Sakai T, Ohshiro K, Yamamoto T: Phenotypic modulation of parietal epithelial cells of Bowman's capsule in culture. Cell Tissue Res 2001, 304:339–349
18. Nyati S, Schinske K, Ray D, Nyati MK, Ross BD, Rehemtulla A: Molecular imaging of TGFbeta-induced Smad2/3 phosphorylation reveals a role for receptor tyrosine kinases in modulating TGFbeta signaling. Clin Cancer Res 2011, 17:7424–7439
19. Hammerschmidt E, Loeffler I, Wolf G: Morg1 heterozygous mice are protected from acute renal ischemia-reperfusion injury. Am J Physiol Renal Physiol 2009, 297:F1273–F1287
20. Klein G, Langegger M, Timpl R, Ekblom P: Role of laminin A chain in the development of epithelial cell polarity. Cell 1988, 55:331–341
21. Sorokin LM, Conzelmann S, Ekblom P, Battaglia C, Aumailley M, Timpl R: Monoclonal antibodies against laminin A chain fragment E3 and their effects on binding to cells and proteoglycan and on kidney development. Exp Cell Res 1992, 201:137–144
22. Abrahamson DR, St John PL: Loss of laminin epitopes during glomerular basement membrane assembly in developing mouse kidneys. J Histochem Cytochem 1992, 40:1943–1953

23. Miner JH: Developmental biology of glomerular basement membrane components. Curr Opin Nephrol Hypertens 1998, 7:13–19
24. Peutz-Kootstra CJ, Hansen K, De Heer E, Abrass CK, Bruijn JA: Differential expression of laminin chains and anti-laminin autoantibodies in experimental lupus nephritis. J Pathol 2000, 192: 404–412
25. Abrahamson DR, Prettyman AC, Robert B, St John PL: Laminin-1 reexpression in Alport mouse glomerular basement membranes. Kidney Int 2003, 63:826–834
26. St John PL, Wang R, Yin Y, Miner JH, Robert B, Abrahamson DR: Glomerular laminin isoform transitions: errors in metanephric culture are corrected by grafting. Am J Physiol Renal Physiol 2001, 280: F695–F705
27. Kashtan CE, Kim Y, Lees GE, Thorner PS, Virtanen I, Miner JH: Abnormal glomerular basement membrane laminins in murine, canine and human Alport syndrome: aberrant laminin alpha2 deposition is species-independent. J Am Soc Nephrol 2001, 12:252–260
28. Cosgrove D, Rodgers K, Meehan D, Miller C, Bovard K, Gilroy A, Gardner H, Kotelianski V, Gotwals P, Amatucci A, Kalluri R: Integrin alpha1beta1 and transforming growth factor-beta1 play distinct roles in Alport glomerular pathogenesis and serve as dual targets for metabolic therapy. Am J Pathol 2000, 157: 1649–1659
29. Lan HY, Chung AC: TGF-beta/Smad signaling in kidney disease. Semin Nephrol 2012, 32:236–243
30. Ziyadeh FN: Different roles for TGF-beta and VEGF in the pathogenesis of the cardinal features of diabetic nephropathy. Diabetes Res Clin Pract 2008, 82(Suppl 1):S38–S41
31. Ziyadeh FN, Sharma K, Ericksen M, Wolf G: Stimulation of collagen gene expression and protein synthesis in murine mesangial cells by high glucose is mediated by autocrine activation of transforming growth factor-beta. J Clin Invest 1994, 93:536–542
32. Yoshioka K, Takemura T, Murakami K, Okada M, Hino S, Miyamoto H, Maki S: Transforming growth factor-beta protein and mRNA in glomeruli in normal and diseased human kidneys. Lab Invest 1993, 68:154–163
33. Inman GJ, Nicolas FJ, Callahan JF, Harling JD, Gaster LM, Reith AD, Laping NJ, Hill CS: SB-431542 is a potent and specific inhibitor of transforming growth factor-beta superfamily type I activin receptor-like kinase (ALK) receptors ALK4, ALK5, and ALK7. Mol Pharmacol 2002, 62:65–74
34. Heldin CH, Miyazono K, ten Dijke P: TGF-beta signalling from cell membrane to nucleus through SMAD proteins. Nature 1997, 390: 465–471
35. Kikkawa R, Togawa M, Isono M, Isshiki K, Haneda M: Mechanism of the progression of diabetic nephropathy to renal failure. Kidney Int Suppl 1997, 62:S39–S40
36. Chai Q, Krag S, Miner JH, Nyengaard JR, Chai S, Wogensen L: TGF-beta1 induces aberrant laminin chain and collagen type IV isotype expression in the glomerular basement membrane. Nephron Exp Nephrol 2003, 94:e123–e136
37. Falk RJ, Scheinman JI, Mauer SM, Michael AF: Polyantigenic expansion of basement membrane constituents in diabetic nephropathy. Diabetes 1983, 32(Suppl 2):34–39
38. Adler S: Structure-function relationships associated with extracellular matrix alterations in diabetic glomerulopathy. J Am Soc Nephrol 1994, 5:1165–1172
39. Mauer SM, Steffes MW, Ellis EN, Sutherland DE, Brown DM, Goetz FC: Structural-functional relationships in diabetic nephropathy. J Clin Invest 1984, 74:1143–1155
40. Alsaad KO, Herzenberg AM: Distinguishing diabetic nephropathy from other causes of glomerulosclerosis: an update. J Clin Pathol 2007, 60:18–26
41. Mason RM, Wahab NA: Extracellular matrix metabolism in diabetic nephropathy. J Am Soc Nephrol 2003, 14:1358–1373
42. Dai C, Liu Y: Hepatocyte growth factor antagonizes the profibrotic action of TGF-beta1 in mesangial cells by stabilizing Smad transcriptional corepressor TGIF. J Am Soc Nephrol 2004, 15:1402–1412
43. Schnaper HW, Kopp JB, Poncelet AC, Hubchak SC, Stetler-Stevenson WG, Klotman PE, Kleinman HK: Increased expression of extracellular matrix proteins and decreased expression of matrix proteases after serial passage of glomerular mesangial cells. J Cell Sci 1996, 109(Pt 10):2521–2528
44. Schnaper HW, Hayashida T, Poncelet AC: It's a Smad world: regulation of TGF-beta signaling in the kidney. J Am Soc Nephrol 2002, 13:1126–1128
45. Higaki Y, Schullery D, Kawata Y, Shnyreva M, Abrass C, Bomsztyk K: Synergistic activation of the rat laminin gamma1 chain promoter by the gut-enriched Kruppel-like factor (GKLF/KLF4) and Sp1. Nucleic Acids Res 2002, 30:2270–2279
46. ten Dijke P, Miyazono K, Heldin CH: Signaling inputs converge on nuclear effectors in TGF-beta signaling. Trends Biochem Sci 2000, 25:64–70
47. Di Guglielmo GM, Le Roy C, Goodfellow AF, Wrana JL: Distinct endocytic pathways regulate TGF-beta receptor signalling and turnover. Nat Cell Biol 2003, 5:410–421
48. Feng XH, Derynck R: Specificity and versatility in tgf-beta signaling through Smads. Annu Rev Cell Dev Biol 2005, 21:659–693
49. Border WA, Noble NA, Yamamoto T, Harper JR, Yamaguchi Y, Pierschbacher MD, Ruoslahti E: Natural inhibitor of transforming growth factor-beta protects against scarring in experimental kidney disease. Nature 1992, 360:361–364
50. Thannickal VJ, Lee DY, White ES, Cui Z, Larios JM, Chacon R, Horowitz JC, Day RM, Thomas PE: Myofibroblast differentiation by transforming growth factor-beta1 is dependent on cell adhesion and integrin signaling via focal adhesion kinase. J Biol Chem 2003, 278: 12384–12389
51. Gullberg D, Ekblom P: Extracellular matrix and its receptors during development. Int J Dev Biol 1995, 39:845–854
52. Shi W, Sun C, He B, Xiong W, Shi X, Yao D, Cao X: GADD34-PP1c recruited by Smad7 dephosphorylates TGFbeta type I receptor. J Cell Biol 2004, 164:291–300